Int. J. Appl. Math. Comput. Sci., 2015, Vol. 25, No. 1, 159–174
DOI: 10.1515/amcs-2015-0012

amcs

SYSTEMATIC FAULT TOLERANT CONTROL BASED ON ADAPTIVE THAU OBSERVER ESTIMATION FOR QUADROTOR UAVs

ZHAOHUI CEN[a], HASSAN NOURA[b,*], YOUNES AL YOUNES[c,d]

[a]Qatar Environment and Energy Research Institute, Member of the Qatar Foundation
Building CP4, Education City, Doha, 5825 Qatar
e-mail: cenzhaohui@gmail.com

[b]Department of Electrical Engineering
United Arab Emirates University, PO Box 15551, Al Ain, UAE
e-mail: hnoura@uaeu.ac.ae

[c]Mechanical Engineering Department
Higher College of Technology, PO Box 17155, Al Ain, UAE
e-mail: yalyounes@hct.ac.ae

[d]Modeling, Information and System Lab, Control and Vehicle Group
University of Picardie Jules Verne, Chemin du Thil, 80000, Amiens, France

A systematic fault tolerant control (FTC) scheme based on fault estimation for a quadrotor actuator, which integrates normal control, active and passive FTC and fault parking is proposed in this paper. Firstly, an adaptive Thau observer (ATO) is presented to estimate the quadrotor rotor fault magnitudes, and then faults with different magnitudes and time-varying natures are rated into corresponding fault severity levels based on the pre-defined fault-tolerant boundaries. Secondly, a systematic FTC strategy which can coordinate various FTC methods is designed to compensate for failures depending on the fault types and severity levels. Unlike former stand-alone passive FTC or active FTC, our proposed FTC scheme can compensate for faults in a way of condition-based maintenance (CBM), and especially consider the fatal failures that traditional FTC techniques cannot accommodate to avoid the crashing of UAVs. Finally, various simulations are carried out to show the performance and effectiveness of the proposed method.

Keywords: systematic fault tolerant control, fault estimation, adaptive Thau observer, fault tolerant capacity boundaries, time-varying fault.

1. Introduction

Due to the recent advances in sensing, communication, computing, and control technologies, unmanned aerial vehicles (UAVs) have become vitally important in many engineering applications and our life, e.g., in surveillance, search and rescue (Pedro *et al*., 2013; Freddi *et al*., 2012; Chamseddine *et al*., 2012). As an example of UAV systems, the quadrotor helicopter is a relatively simple, affordable and easy to fly system and thus it has been widely used to develop, implement and test-fly methods in control, fault diagnosis, fault tolerant control (FTC) as well as multi-agent based technologies in formation flight, cooperative control, distributed control, mobile wireless networks and communications (Zhang and Chamseddine, 2012; Bouadi *et al*., 2007).

Many works on FTC of quadrotors have been recently proposed in the event of a failure in some of their components, which can be classified into passive FTC (PFTC) and active FTC (AFTC) (Zhang and Jiang, 2008; 2003). PFTC techniques can tolerate a predefined set of faults by using a specially designed fixed controller. Berbra *et al*. (2008), Khebbache *et al*. (2012), Li *et al*. (2011), Montes de Oca *et al*. (2012), Khelassi *et al*. (2011), Theilliol *et al*. (2008) and Boussaid *et al*. (2011) proposed some passive FTC schemes based on classical control methods such as sliding-mode control, backstepping control, or model adaptive control. These PFTC controllers can compensate for faults and

*Corresponding author

disturbances in both fault-free and faulty conditions. However, a disadvantage is that only specific faults can be tolerated and the fault magnitude should not exceed given boundaries.

AFTC techniques rely on the fault detection and diagnosis (FDD) process to monitor system performance and to identify and detect faults in the system, and the controller parameters are reconfigured on-line. In consequence, they are more flexible than PFTC ones and can compensate for faults with a large magnitude which cannot be compensated by PFTC. Some works have dealt with AFTC of quadrotors (Ranjbaran and Khorasani, 2010; Izadi *et al*., 2011; Sadeghzadeh *et al*., 2011; Yang *et al*., 2012; Fang and Blanke, 2011; Edwards *et al*., 2012). In those AFTC approaches with fault estimation and adaptive fault compensation (Jiang *et al.*, 2011; 2006; Jiang and Chowdhury, 2005), the fault is diagnosed first and then the controller or actuator output is incremented based on the fault estimation result in order to compensate for the fault.

A drawback of these AFTC techniques is that not only a serious fault case but also slight fault cases are compensated for by a complex-structure AFTC. In fact, although AFTC is applicable for both the slight-fault and severe fault scenarios, it is not necessary to apply AFTC to slight fault cases because it wastes some resources, especially the actuator resources. In addition to that, it may not obviously result in better control performance than normal control and PFTC. More importantly, neither PFTC nor AFTC can tolerate faults with an infinitely large value, and in the worst case, where the accommodation controller fails, neither safety measures nor an effective fault-parking method is taken to avoid the breaking down and crash of the quadrotor. Therefore, it is essential to consider the fault-tolerant capacity of different control approaches based on the availability of high-accuracy fault estimation (FE), and apply the most suitable FTC controller into the corresponding fault cases, as well as introduce an effective safety measure in case all FTC approaches did not perform well.

Fault-parking is derived from a recently proposed concept of safety-parking in the research area of industry safety and reliability (Du and Mhaskar, 2011; Du *et al.*, 2011; Gandhi and Mhaskar, 2009; 2008; Mahmood *et al.*, 2008). This means that safety measures, in an economical way, are advised to be taken when an absolute recovery is impossible. The normal operation mode or profile will be replaced by a relatively safe but simple one. Especially for aircraft flight control applications, it is strongly suggested to let the aircraft land and park when the failures are not recoverable or FTC also fails.

The contribution of this paper is that fault-tolerant capabilities of different FTC techniques are innovatively analyzed and addressed based on our former research outcome on fault estimation using the adaptive Thau observer (ATO) (Zhaohui *et al.*, 2013a; 2013b; 2013c). Also, a simple fault parking measure is introduced to avoid fatal failures of quadrotor FTC approaches. Aimed at the applicability boundary of different FTCs, a systematic FTC strategy made up of normal control, PFTC, AFTC and safe fault parking is proposed to control the quadrotor in a flexible way according to the fault estimation result. Unlike former stand-alone FTC approaches, our systematic FTC strategy can match the optional controller well with the corresponding fault cases and can improve the reliability and performance of the quadrotor comprehensively. Compared with our former research on FE and FTC of a quadrotor (Zhaohui and Noura, 2013a; 2013b), this paper proposes a systematic FTC strategy with the fault-parking concept and integrates the ATO fault estimation and systematic FTC scheme as a complete unit.

This paper is organized as follows. In Section 2, some issues about the nonlinear model of a quadrotor UAV, fault severity estimation and fault tolerant control efficiency are presented and discussed. The adaptive Thau observer used for fault estimation is introduced in Section 3. The proposed systematic FTC scheme is discussed in Section 4. Section 5 is devoted to the presentation of simulation results obtained for various fault-free situations and fault scenarios when the proposed scheme is applied to the quadrotor UAV. Finally, a conclusion is provided in Section 6.

2. Problem formulation

2.1. Quadrotor model. The dynamic model can be derived from the Euler–Lagrange formalism. There are two reference frames for its dynamic model, which are named a body-fixed frame B and an earth-fixed frame E, as depicted in Fig. 1 (Freddi *et al.*, 2012). Both of them are assumed to be at the center of gravity of the quadrotor UAV.

The position of the quadrotor in the earth frame E is defined as x, y, z. The attitude of a quadrotor, such as roll, pitch, and yaw, is denoted by ϕ, θ, ψ with respect to the frame B. Analytical models are a basis for research on the control of quadrotors. The most popular model is provided in the form

$$\begin{aligned} m\ddot{x} &= u_z\left(\cos\phi\sin\theta\cos\psi + \sin\phi\sin\psi\right) - k_x\dot{x},\\ m\ddot{y} &= u_z\left(\cos\phi\sin\theta\sin\psi - \sin\phi\cos\psi\right) - k_y\dot{y},\\ m\ddot{z} &= u_z\left(\cos\phi\cos\theta\right) - mg - k_z\dot{z},\\ J_x\dot{p} &= u_p + (J_y - J_z)qr - J_T q\Omega - k_p p,\\ J_y\dot{q} &= u_q + (J_z - J_x)pr - J_T p\Omega - k_q q,\\ J_z\dot{r} &= u_r + (J_x - J_y)pq - k_r r. \end{aligned} \tag{1}$$

which is derived from position dynamics in the inertial frame and the angular dynamics,

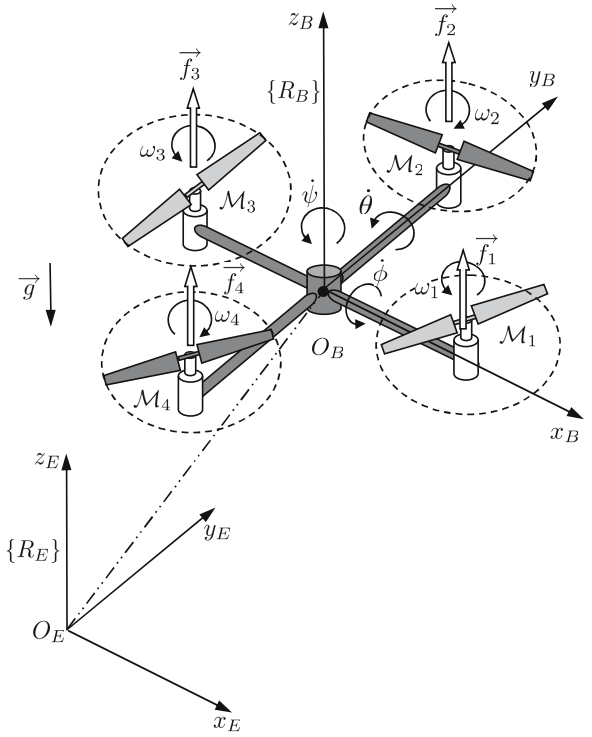

Fig. 1. Quadrotor in different frames.

The angular velocities in the inertial frame (Euler rates) can be related to those in the body frame as follows:

$$\begin{bmatrix} p \\ q \\ r \end{bmatrix} = \begin{bmatrix} 1 & 0 & -\sin\theta \\ 0 & \cos\phi & \cos\theta\sin\phi \\ 0 & -\sin\phi & \cos\theta\cos\phi \end{bmatrix} \begin{bmatrix} \dot{\phi} \\ \dot{\theta} \\ \dot{\psi} \end{bmatrix} = \begin{bmatrix} \dot{\phi} \\ \dot{\theta} \\ \dot{\psi} \end{bmatrix}. \quad (2)$$

Close to hovering conditions, the matrix in the above equation is close to the identity matrix and therefore the angular velocities in the body frame can be seen as the angular velocities in the inertial frame. The model can then be written as

$$\begin{aligned} m\ddot{x} &= u_z \cos\phi \sin\theta \cos\psi + \sin\phi \sin\psi - k_x \dot{x}, \\ m\ddot{y} &= u_z \left(\cos\phi \sin\theta \sin\psi - \sin\phi \cos\psi\right) - k_y \dot{y}, \\ m\ddot{z} &= u_z \left(\cos\phi \cos\theta\right) - mg - k_z \dot{z}, \\ J_x\ddot{\theta} &= u_\theta + (J_y - J_z)\dot{\phi}\dot{\psi} - J_T\dot{\phi}\Omega - k_\theta\dot{\theta}, \\ J_y\ddot{\phi} &= u_q + (J_z - J_x)\dot{\theta}\dot{\psi} - J_T\dot{\theta}\Omega - k_\phi\dot{\phi}, \\ J_z\ddot{\psi} &= u_\psi + (J_x - J_y)\dot{\theta}\dot{\phi} - k_\psi\dot{\psi}, \end{aligned} \quad (3)$$

where u_p, u_q, u_r, k_p, k_q and k_r have been respectively changed to u_θ, u_ϕ, u_ψ, k_θ, k_ϕ, k_ψ for notational convenience. The system inputs U_1, U_2, U_3, U_4 are defined as follows:

$$\begin{aligned} U_1 &= b\left(\omega_4^2 - \omega_2^2\right) = F_4 - F_2, \\ U_2 &= b\left(\omega_3^2 - \omega_1^2\right) = F_3 - F_1, \\ U_3 &= d\left(\omega_1^2 + \omega_3^2 - \omega_2^2 - \omega_4^2\right), \\ U_4 &= b\left(\omega_1^2 + \omega_2^2 + \omega_3^2 + \omega_4^2\right) = \sum_{i=1}^{4} F_i, \end{aligned} \quad (4)$$

where b and d are the thrust and drag coefficients, respectively, and $\omega = \omega_4 + \omega_3 - \omega_2 - \omega_1$ is considered a disturbance. The relationship between system inputs and the speed of rotors can be given in the matrix form as follows:

$$\begin{aligned} \begin{bmatrix} U_1 \\ U_2 \\ U_3 \\ U_4 \end{bmatrix} &= \begin{bmatrix} 0 & -b & 0 & b \\ -b & 0 & b & 0 \\ d & -d & d & -d \\ b & b & b & b \end{bmatrix} \begin{bmatrix} \omega_1^2 \\ \omega_2^2 \\ \omega_3^2 \\ \omega_4^2 \end{bmatrix} \\ &= \Omega \begin{bmatrix} \omega_1^2 \\ \omega_2^2 \\ \omega_3^2 \\ \omega_4^2 \end{bmatrix}. \end{aligned} \quad (5)$$

Since Ω is nonsingular, it is obvious that for each U_i we can find appropriate $\omega_j^2, j = 1, \ldots, 4$ while the other inputs $U_k, k \neq i$ do not change. Defining

$$x^T = \left(\phi, \theta, \psi, \dot{\varphi}, \dot{\theta}, \dot{\psi}\right)$$

as the state vector,

$$u = \begin{bmatrix} U_\phi & U_\theta & U_\psi \end{bmatrix}^T$$

as the input vector and

$$y = \begin{bmatrix} \phi & \theta & \psi \end{bmatrix}^T$$

as the output vector, the system described in (1) can be rewritten in the state-space form $\dot{x} = f(x, u)$ as

$$\begin{cases} \dot{x}(t) = Ax(t) + Bu(t) + H(x(t), u(t)), \\ y(t) = Cx(t), \end{cases} \quad (6)$$

where $H(x, u) = \begin{bmatrix} 0 & 0 & 0 & h(x, u)^T \end{bmatrix}^T$ and

$$h(x, u) = \begin{bmatrix} \dot{\psi}\dot{\theta}\left(I_y - I_z/I_x\right) \\ \dot{\phi}\dot{\psi}\left(I_z - I_x/I_y\right) \\ \dot{\theta}\dot{\phi}\left(I_x - I_y/I_z\right) \end{bmatrix}. \quad (7)$$

2.2. Fault severity estimation. When dealing with nonlinear model-based techniques, there are two possible approaches: linearizing the system around different operating points or using a nonlinear model-based approach (Freddi *et al.*, 2009). Generally, a nonlinear observer is used for modeling and observing the nonlinear system. In order to design the nonlinear observer, the system described by (3) need be denoted in a new state-space form. Defining

$$x^T = \left(x, y, z, \phi, \theta, \psi, \dot{x}, \dot{y}, \dot{z}, \dot{\phi}, \dot{\theta}, \dot{\psi}\right)$$

as the new state vector, the system described in (3) can be rewritten as

$$\begin{cases} \dot{x}(t) = Ax(t) + Bu(t) + H(x(t), u(t)), \\ y(t) = Cx(t), \end{cases} \quad (8)$$

where

$$u = \begin{bmatrix} U_T & U_\phi & U_\theta & U_\psi \end{bmatrix}^T,$$
$$y = \begin{bmatrix} x & y & z & \phi & \theta & \psi \end{bmatrix}^T,$$
$$H(x,u) = \begin{bmatrix} 0 & 0 & 0 & 0 & 0 & 0 & 0 \\ 0 & 0 & h^T(x,u) \end{bmatrix}^T,$$

and

$$h(x,u) = \begin{bmatrix} C_\phi C_\psi S_\theta + S_\phi S_\psi \\ C_\phi S_\theta S_\psi - C_\psi S_\phi \\ (C_\theta C_\phi) \end{bmatrix} u - \begin{bmatrix} 0 \\ 0 \\ g \end{bmatrix}. \quad (9)$$

When a fault occurs in the actuators, the fault system can be described by (10), which derives from (8). A candidate observer for this kind of nonlinear system is the observer proposed by Thau (Chen and Patton, 1999). The Thau observer has already been applied for fault detection and isolation of nonlinear dynamic systems. It uses the following nonlinear system model:

$$\begin{cases} \dot{x}(t) = Ax(t) + Bu(t) + H(x(t), u(t)) + Ff(t), \\ y(t) = Cx(t), \end{cases} \quad (10)$$

where F is known as the fault entry matrix, which represents the fault position, and $f(t)$ denotes the time-varying fault offset signal. In consequence, in order to design and implement an active FTC approach for quadrotors, it is essential to propose a solution for detecting the fault and estimating its value f in (10).

2.3. Fault-tolerant efficiency. With reference to the quadrotor model (3), the control laws such as PID control, backstepping control, or sliding-mode control could b employed to track the reference attitude and position, and stabilize the quadrotor. Normally, the controller should be more or less robust to noise, disturbance and uncertainty. Besides, it is also robust to some faults with slight severity because the fault can be seen as a disturbance. But if the fault magnitude exceeds a certain range, the system will lose control and become unstable. Thus, in this case, some fault-tolerant problems should be considered:

1. How to diagnose the fault and estimate its severity?
2. What is the range for the fault magnitude or the fault-tolerant capacity and how to get them?
3. How to compensate for the fault by using a freely-switched controller between PFTC and AFTC instead of a single fixed controller for fault-tolerant efficiency?

3. Fault diagnosis and severity estimation

In order to implement FD and FE separately, a fault diagnosis scheme based on two Thau observers is proposed to detect and estimate the fault severity. First, the original Thau observer is used to detect faults based on residual generation and evaluation. Then, an adaptive Thau observer is proposed and designed for fault estimation based on the observer gain. The fault detection and estimation process is depicted in Fig. 2.

3.1. Fault detection based on the Thau observer. The following conditions must be satisfied for the observer design:
$C1$: The pair (C, A) is observable,
$C2$: The function $h(x, u)$ must be continuously differentiable and locally Lipschitz with constant $\rho > 0$, i.e.,

$$\|h(x_1(t), u(t)) - h(x_2(t), u(t))\| \le \rho \|(x_1 - x_2)\|. \quad (11)$$

If these two conditions are satisfied, a nonlinear Thau observer can be built as

$$\begin{cases} \dot{\hat{x}}(t) = A\hat{x}(t) + Bu(t) + H(\hat{x}(t), u(t)) \\ \qquad\quad + K(y(t) - \hat{y}(t)), \\ \hat{y}(t) = C\hat{x}(t), \end{cases} \quad (12)$$

where $\hat{x}(t) \in \mathbb{R}^n$ is the observer state vector, $\hat{y}(t) \in \mathbb{R}^p$ is the observer output vector. K is the observer feedback gain matrix, and is designed according to the conditions in Theorem 1.

Theorem 1. (Chen and Patton, 1999, Thm. 9, p. 256) *If the gain matrix K in* (12) *satisfies*

$$K = {P_\theta}^{-1} C^T \quad (13)$$

and the matrix P_θ is the solution of

$$A^T P_\theta + P_\theta A - C^T C + \theta C^T P_\theta = 0, \quad (14)$$

where θ is a positive parameter such that (14) *has a positive definite solution, then the state of* (12) *is an asymptotic estimate of the system state described by* (8)*, i.e.,*

$$\lim_{t\to\infty} e(t) = \lim_{t\to\infty} (x(t) - \hat{x}(t)) = 0. \quad (15)$$

If a fault occurs, the observer will not track the system states again; the residual $e_y(t) = y(t) - \hat{y}(t)$ will deviate from zero indicating the presence of a fault.

3.2. Fault estimation based on an adaptive Thau observer. Based on the fault detection result from the Thau observer, an adaptive Thau observer is proposed to

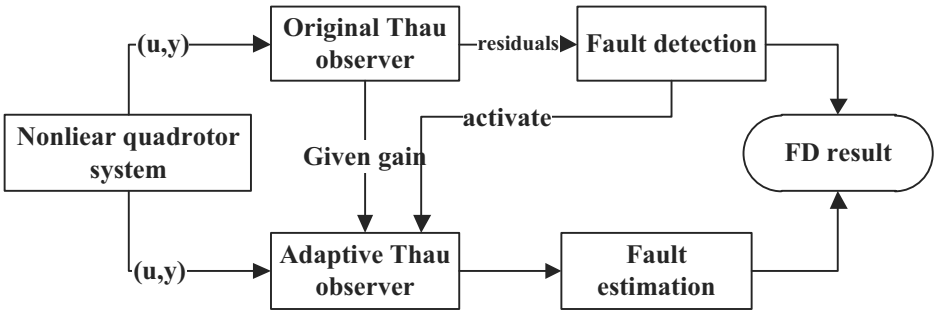

Fig. 2. FD scheme for the quadrotor.

estimate the fault severity. With reference to (11) and (13), a novel Thau observer can be constructed as

$$\begin{aligned}\dot{\hat{x}}(t) &= A\hat{x}(t) + Bu(t) + H(\hat{x}(t), u(t)) \\ &\quad + F\hat{f}(t) + K(y(t) - \hat{y}(t)), \\ \hat{y}(t) &= C\hat{x}(t),\end{aligned} \tag{16}$$

where $\hat{f}(t)$ is an estimate of $f(t)$, $K \in \mathbb{R}^{n\times p}$ is the observer feedback gain.

Denoting the estimation error by $e_x(t) = x(t) - \hat{x}(t)$, the error dynamics are described by

$$\dot{e}_x(t) = (A - KC)e_x(t) + [H(x) - H(\hat{x})] + Fe_f(t), \tag{17}$$

where the fault estimation error is denoted by $e_f(t) = f(t) - \hat{f}(t)$.

The purpose of the proposed adaptive Thau observer is not only to detect faults, but also to estimate the fault parameters, which can be used for fault accommodation.

Theorem 2. *For the available observer gain K in Theorem 1 as well as a matrix $Q_{(n\times n)} > 0$ and a positive parameter γ, if there exist two matrices $P_{n\times n}$ and $G_{r\times p}$ satisfying*

$$P(A - KC) + (A - KC)^T P + \gamma PP + \gamma I = -Q, \tag{18}$$

$$PB = C^T G^T, \tag{19}$$

then the observer given in (16) *with the adaptive fault estimation law (Meng et al., 2009; Zhang et al., 2007):*

$$\dot{\hat{f}}(t) = \Gamma G(y(t) - \hat{y}(t)) - \sigma\Gamma\hat{f}(t) \tag{20}$$

can lead to

$$\lim_{t\to\infty} e_x(t) = 0, \quad \lim_{t\to\infty} e_f(t) = 0,$$

where $\Gamma = \Gamma^T > 0$ is a weighing matrix, σ is positive constant which satisfies $\sigma - \lambda_{\max}(\Gamma^{-1}) > 0$, $\lambda_{\max}(\cdot)$ is the maximum eigenvalue of the corresponding matrix.

Proof. From $e_f(t) = f(t) - \hat{f}(t)$, we get

$$\dot{e}_f = \dot{f} - \Gamma G e_y + \sigma\Gamma f - \sigma\Gamma e_f. \tag{21}$$

For the Lyapunov function

$$V(t) = e_x^T P e_x + e_f^T \Gamma^{-1} e_f \tag{22}$$

we have

$$\begin{aligned}\dot{V} &= e_x^T \left[(A - LC)^T P + P(A - LC)\right] e_x \\ &\quad + 2e_x^T P\left[H(x) - H(\hat{x})\right] \\ &\quad + 2e_f^T \Gamma^{-1}\dot{f} + 2\sigma e_f^T f - 2\sigma e_f^T e_f \\ &\le e_x^T \left[(A - LC)^T P + P(A - LC) + \gamma PP + \gamma I\right] e_x \\ &\quad + \lambda_{\max}\left(\Gamma^{-1}\right)\left[\|e_f\|^2 + f_1^2\right] \\ &\quad + \sigma\left[\|e_f\|^2 + f_0^2\right] - 2\sigma\|e_f\|^2 \\ &\le -\lambda_{\min}(Q)\|e_x\|^2 - \left[\sigma - \lambda_{\max}(\Gamma^{-1})\right]\|e_f\|^2 \\ &\quad + \lambda_{\max}\left(\Gamma^{-1}\right)\cdot f_1^2 + \sigma f_0^2 \\ &= -\lambda_{\min}(Q)\|e_x\|^2 - \left[\sigma - \lambda_{\max}(\Gamma^{-1})\right]\|e_f\|^2 + \beta,\end{aligned} \tag{23}$$

where $\beta = \lambda_{\max}\left(\Gamma^{-1}\right)\cdot f_1^2 + \sigma f_0^2$, $\lambda_{\min}(\cdot)$ is the minimum eigenvalue of the matrix. If the appropriate parameters satisfy

$$\sigma - \lambda_{\max}(\Gamma^{-1}) > 0, \tag{24}$$

then $\dot{V}$ can be obtained as

$$\begin{aligned}\dot{V} \le &-\min\left[\lambda_{\min}(Q), \sigma - \lambda_{\max}(\Gamma^{-1})\right] \\ &\times\left(\|e_x\|^2 + \|e_f\|^2\right) + \beta,\end{aligned} \tag{25}$$

Moreover, based on $V(t) = e_x^T P e_x + e_f^T \Gamma^{-1} e_f$, the following can be obtained:

$$V \le \max\left[\lambda_{\max}(P), \lambda_{\max}\left(\Gamma^{-1}\right)\right]\left(\|e_x\|^2 + \|e_f\|^2\right). \tag{26}$$

Thus

$$\dot{V} \leq -\alpha V + \beta, \tag{27}$$

where

$$\alpha = \frac{\min\left[\lambda_{\min}\left(Q\right), \sigma - \lambda_{\max}(\Gamma^{-1})\right]}{\max\left[\lambda_{\max}\left(P\right), \lambda_{\max}\left(\Gamma^{-1}\right)\right]}.$$

The differential inequality (27) satisfies

$$0 \leq V(t) \leq \frac{\beta}{\alpha} + \left[V\left(0\right) - \frac{\beta}{\alpha}\right] e^{-\alpha t},$$

so, as $t \to \infty$, $V(t)$ is uniformly ultimately bounded. Therefore, the adaptive Thau observer is asymptotically stable, and e_f is also uniformly and ultimately bounded. The ultimate norm bound of e_f is

$$\|e_f\| \leq \sqrt{\frac{\beta}{\alpha\lambda_{\min}(\Gamma^{-1})}}. \tag{28}$$

This completes the proof. ■

Remark 1. Theorem 2 is theoretically suitable for all faults with different time-varying natures. However, it should be pointed out that the estimation convergence speed depends both on the fault time-varying nature and the specified parameters of the ATO. Hereby, as can be seen from (21), a suitable value of Γ and σ should be set for better estimation performance subjected to faults with different time-varying natures. If the fault vector$f(t)$is constant or its derivative is close to zero, we can obtain another adaptive observer in a simplified form according to Theorem 2.

Theorem 3. *If the fault $f(t)$ is constant and the adaptive fault estimation law is in the form of* (29)*, $\dot{V} < 0$ will be satisfied and the proposed adaptive Thau observer is asymptotically stable based on the Lyapunov theorem:*

$$\dot{\hat{f}} = \Gamma G(\hat{y}(t) - y(t)). \tag{29}$$

Proof. Consider the same Lyapunov function of (25). Then its derivative satisfies

$$\dot{V} \leq -e_x^T Q e_x \leq -\lambda_{\min}(Q)\|e_x\|^2 \leq 0. \tag{30}$$

This completes the proof. ■

4. Fault tolerant control for the quadrotor

In this section, a systematic FTC scheme based on fault estimation is designed to address the three problems of fault-tolerant efficiency mentioned in Section 2. Firstly, the fault-tolerant capacity is discussed and defined for fault severity level classification. Then, a systematic FTC controller including normal control, PFTC, AFTC and fault parking is designed to compensate faults in different conditions.

4.1. Fault severity assessment based on fault-tolerant capacity. After the fault magnitude is obtained by the ATO, a fault severity assessment rule is designed to classify the fault into different levels. In order to invoke corresponding FTC control, four control strategies are considered to compensate for the faults in different levels, as it can be seen in Fig. 3.

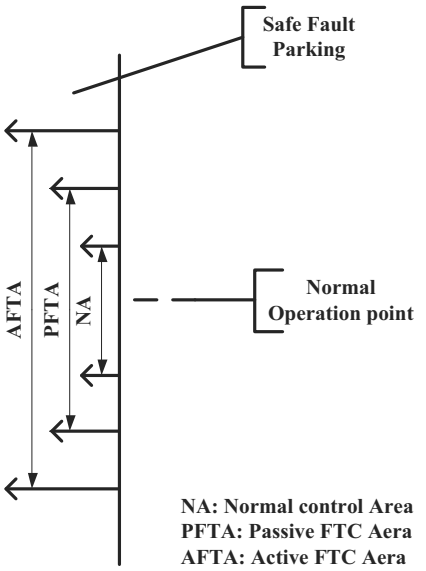

Fig. 3. Fault severities classification and the corresponding FTC strategy.

The first level is the NA (normal control area) level, which means the fault-tolerance capacity that a normal controller has in case no measures are taken when faults occur.

The second level is the PFTA (passive FTC area) level, which means the fault-tolerance capacity that a passive FTC has when a predefined fault-tolerant controller is set for some faults at the beginning.

The third level is the AFTA (active FTC area) level, which means the fault-tolerance capacity that an active FTC has when an FE based fault-tolerant controller is set for faults.

The fourth level is the safe fault parking level. In this case, the primary control objective for the quadrotor is to slow down the velocities and have a safe landing in stable mode.

The upper and low bound value of the AFTA, PFTA and NA can be obtained based on numerical simulations in a limited number of discontinuous fault values.

4.2. Systematic FTC strategies. According to the four fault severity levels above, four control strategies are

designed and switched on based on the fault estimation result.

4.2.1. Normal controller. A PD controller is introduced for each orientation angle:

$$U_{2,3,4} = k_{\phi,\theta,\psi}(\phi,\theta,\psi) + d_{\phi,\theta,\psi}(\phi,\theta,\psi). \tag{31}$$

If the PD controller is used in each loop, the dynamics model of each close-loop will be a second order system. Here we have

$$\begin{aligned} \Phi &= \frac{K}{s^2}\left[K_p\Phi_d - (K_p + sK_d)\,\Phi\right] \\ \Rightarrow \quad \frac{\Phi}{\Phi_d} &= \frac{KK_p}{s^2 + sKK_d + KK_p}. \end{aligned} \tag{32}$$

This second order system can be written as

$$\frac{\Phi}{\Phi_d} = \frac{G{w_n}^2}{s^2 + 2\xi w_n s + {w_n}^2}. \tag{33}$$

By identification, we have

$$\begin{aligned} K_p &= \frac{{w_n}^2}{K} \\ K_d &= \frac{2\xi w_n}{K}, \end{aligned} \tag{34}$$

while for position control, we will have

$$U_{x,y} = k_{x,y}(x,y) + d_{x,y}(x,y), \tag{35}$$

$$U_z = k_z(z) + p_z(z) + d_z(z). \tag{36}$$

The x and y controls follow the position by controlling the roll and pitch angels indirectly. The relationship is

$$\begin{cases} \cos\phi\sin\theta = \dfrac{m}{U_z}\ddot{x} = \dfrac{U_\theta}{U_z}, \\ -\sin\phi = \dfrac{m}{U_z}\ddot{y} = \dfrac{U_\varphi}{U_z}, \\ \cos\phi\cos\theta = \dfrac{m}{U_z}(\ddot{z} + g), \end{cases} \tag{37}$$

$$\begin{cases} \theta = \operatorname{atan}\left(\dfrac{\ddot{x}}{\ddot{z} + g}\right), \\ \phi = \operatorname{atan}\left(\dfrac{-\ddot{y}}{\sqrt{\ddot{x}^2 + (\ddot{z} + g)^2}}\right), \\ U_z = -\dfrac{m}{\sin\phi}\,\ddot{y}. \end{cases} \tag{38}$$

4.2.2. Passive FTC controller. For PID control, the controller is generally robust to modeling uncertainty and disturbances. The faults can be also seen as modeling uncertainty or disturbance. Thus, in order to compensate a fault, one way could be by considering the fault-tolerance capacity in the design of controller.

Here gain scheduled based PID control is used to implement passive fault tolerant control. Consider the normal control

$$U_n = k_p(x - x_d) + k_d(\dot{x} - x_d). \tag{39}$$

If the actuator output is subject to a loss in effectiveness, the faulty control input can be denoted by

$$u_f = (1 - f)u_n, \tag{40}$$

where f is the percent of faults compared with the normal actuator output. Consequently, the fault matrix can be denoted by

$$F_{l\times l} = \begin{bmatrix} f_1 & & \\ & \ddots & \\ & & f_l \end{bmatrix}. \tag{41}$$

Therefore, the normal controller can be modified as a new passive FTC control:

$$U_{\mathrm{PFTC}} = (I - F)^{-1}U_n. \tag{42}$$

It should be pointed out that the bound of F must match well the controller stability. The upper and lower bounds of F can be obtained from simulation or theoretical analysis on the closed-loop Bode plot.

4.2.3. Active FTC controller. If the fault magnitude can be estimated, then it will be used by the controller to compensate for the fault effect on the system. Thus, with reference to (39) and (40), the normal control law can be modified as a new active FTC control:

$$U_{\mathrm{AFTC}} = U_n + U_f(\hat{f}), \tag{43}$$

where $\hat{f}$ is the estimate of the fault f, and $U_f(\hat{f})$ is the function of $\hat{f}$, which is the control output offset caused by the fault.

4.2.4. Safe fault parking controller. For quadrotor control, once the ATO has detected that the quadrotor has faced a severe loss in one of its rotors, the control strategy has to be changed to mitigate the effect of the fault. This control strategy is to land the quadrotor safely (Sharifi *et al.*, 2010). If the fault severity exceeds the range of AFTC fault-tolerance capacity and enters into the fault parking area, the fault-parking strategy is adopted to make the system change into a stable state. Once the quadrotor is stable in the hovering condition, vertical landing is executed. Then, the power of the quadrotor is turned off until the quadrotor touches the land in order to avoid crashes. The fault parking control procedure can be seen in Fig. 4.

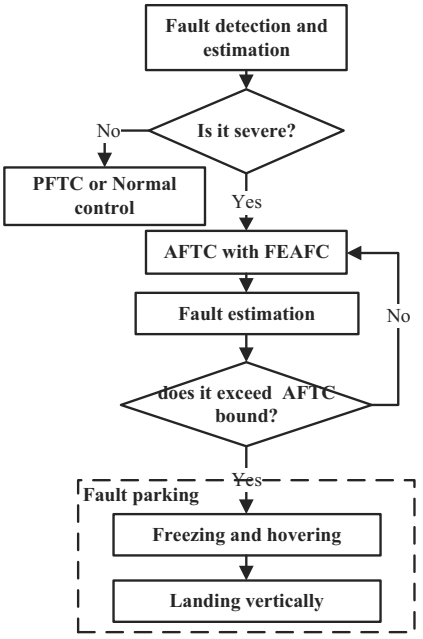

Fig. 4. Fault parking control procedure.

5. Simulation results

In order to show the performance and effectiveness of the proposed method, the nonlinear model of a quadrotor UAV is simulated in the SIMULINK@MATLAB environment. The quadrotor model, whose parameters are identified from a real Pelican quadrotor UAV available in the control lab at UAE University (see Fig. 5), is employed for simulation. The parameters of the

Fig. 5. Pelican quadrotor UAV in the control lab.

quadrotor are $m = 1$ kg, $I_{xx} = 8.1 \times 10^{-3}$ N/m, $I_{yy} = 8.1 \times 10^{-3}$ N/m $I_{zz} = 14.2 \times 10^{-3}$ N/m, $g = 9.81$ N/kg, $J = 1.04 \times 10^{-4}$ N/m.

$$A = \begin{bmatrix} 0_{6\times6} & I_{6\times6} \\ 0_{6\times6} & 0_{6\times6} \end{bmatrix},$$

$$B = \begin{bmatrix} 0_{9\times1} & 0_{9\times3} \\ 0_{3\times1} & I_{3\times3} \end{bmatrix},$$

$$C = \begin{bmatrix} I_{6\times6} & 0_{6\times6} \end{bmatrix}.$$

The parameters of the observers are given below:

$$K = \begin{bmatrix} 1.1 & 0 & 0 & 0 & 0 & 0 \\ 0 & 1.1 & 0 & 0 & 0 & 0 \\ 0 & 0 & 1.1 & 0 & 0 & 0 \\ 0 & 0 & 0 & 1.1 & 0 & 0 \\ 0 & 0 & 0 & 0 & 1.1 & 0 \\ 0 & 0 & 0 & 0 & 0 & 1.1 \\ 0.3205 & 0 & 0 & 0 & 0 & 0 \\ 0 & 0.3205 & 0 & 0 & 0 & 0 \\ 0 & 0 & 0.3205 & 0 & 0 & 0 \\ 0 & 0 & 0 & 0.3205 & 0 & 0 \\ 0 & 0 & 0 & 0 & 0.3205 & 0 \\ 0 & 0 & 0 & 0 & 0 & 0 \end{bmatrix},$$

$$G = \begin{bmatrix} 0 & 0 & 5.38 & 0 & 0 & 0 \\ 0 & 0 & 0 & 5.38 & 0 & 0 \\ 0 & 0 & 0 & 0 & 5.38 & 0 \\ 0 & 0 & 0 & 0 & 0 & 5.38 \end{bmatrix},$$

Γ=I$_4 \times 10^{-8}$, $\sigma = 2 \times 10^8$.

Two sets of simulations are performed to validate the effectiveness of the proposed FE and FTC schemes.

5.1. Fault diagnosis results. In order to validate the FE performance of the proposed ATO for the actuator partial loss of effectiveness (LOE), two fault scenarios were simulated. The fault-free control trajectory of attitude and altitude is shown in Fig. 8. The first fault corresponds to a sine wave offset fault signal with two different frequencies injected into the throttle input, which is the control input for quadrotor altitude control. The other fault corresponds to a sine wave offset fault signal injected into one of the rotors output, which matches well with what the real fault derives from. The relationship between the system inputs and the rotor output is as given by (4) and (5).

5.1.1. Fault scenario 1. Based on the nonlinear state-equations of the quadrotor (10), a sine wave offset fault signal is injected into the throttle input U_1 according to (44). Then the fault matrix is set to $F = [1000]^T$. In order to validate the corresponding response effect for different faults at quickly and slowly time-varying speeds, two frequencies, including $f_1 = 1/5$ Hz and $f_2 = 1/50$

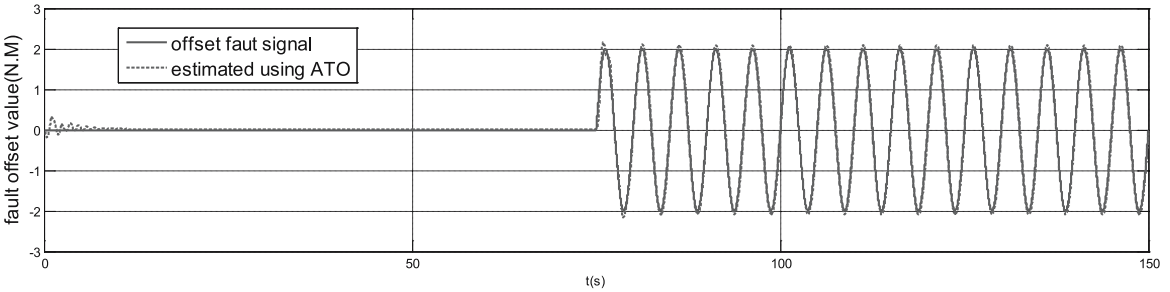

Fig. 6. Fault estimation for $f_1 = 1/5$ Hz.

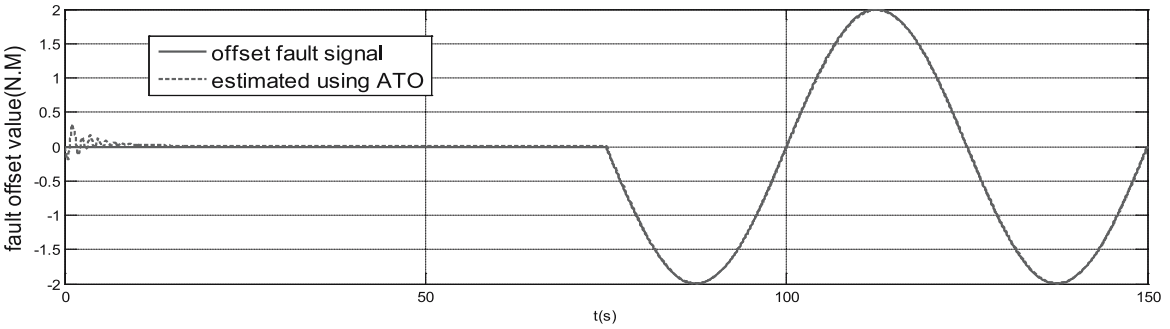

Fig. 7. Fault estimation for $f_2 = 1/50$ Hz.

Hz, are considered:

$$f_1(t) = \begin{cases} 0, & t \in [0, 75), \\ 2\sin\left(\frac{2\pi t}{5}\right), & t \geq 75, \end{cases} \tag{44}$$

$$f_2(t) = \begin{cases} 0, & t \in [0, 75), \\ 2\sin\left(\frac{2\pi t}{50}\right), & t \geq 75. \end{cases} \tag{45}$$

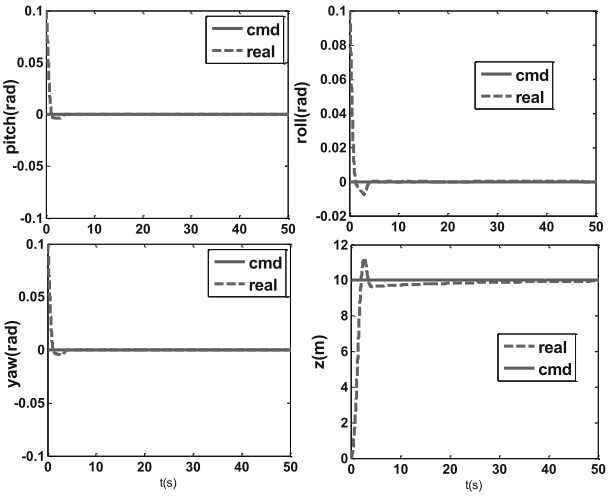

Fig. 8. Fault-free control trajectory of attitude and altitude.

The fault estimation result using the ATO for both cases is shown in Figs. 6 and 7. From the plot comparisons between the offset fault signal and its estimates in Figs. 6 and 7, it can be seen that the ATO exhibits fast convergence performance and high-accuracy for estimation. Although the fault signal has a different time-varying nature, the ATO is effective for both of them. Of course, it is also suitable for constant faults.

Figures 9–11 show comparisons between the fault-free case and the faulty case with time-varying LOE fault $f_2 = 1/50$ Hz for the system output, control output, and rotor output. As can be seen from Figs. 9 and 10, the altitude z and the corresponding control input U_4 change at $t = 75$ s because the fault occurs, while the attitude state and the corresponding control inputs are kept normal. Figure 11 shows that four rotor outputs $F_1 - F_4$ change with same magnitude $U_4/4$ because of an LOE fault in U_4.

5.1.2. Fault scenario 2. The actuators of the quadrotor are actually the four rotors installed in a cross configuration, but they are transformed into Roll, Pitch, Yaw and Throttle command inputs for flight control. Thus it makes more sense to inject the fault into the rotor and then estimate the offset fault value. In order to validate the FE for the partial LOE and time-varying fault in the rotor, a sine wave offset fault signal is injected into the rotors output F_2 as the square of its angular velocity. The sine wave offset fault signal is given by (3). Here it denotes an additional torque to F_2 with the value $T_{\text{add}} = b\omega^2_{\text{offset}}$

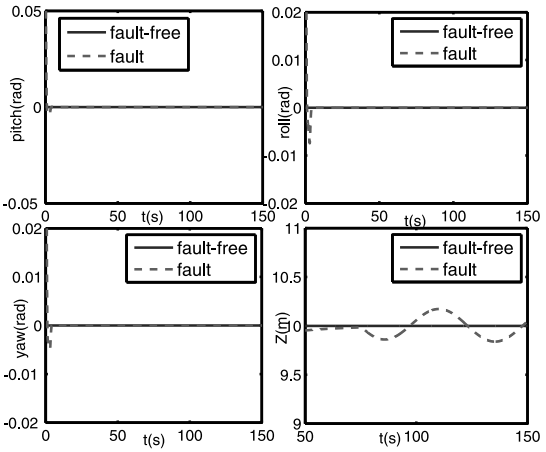

Fig. 9. System outputs in the case of a time-varying LOE fault $f_2 = 1/50$ Hz.

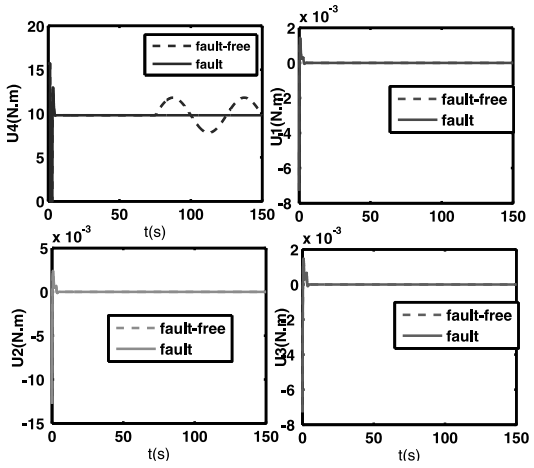

Fig. 10. Controller outputs in the case of a time-varying LOE fault $f_2 = 1/50$ Hz.

because that rotor angular velocity changes.

$$\omega^2_{\text{offset}} = \begin{cases} 0, & t \in [0, 75), \\ 2000 \sin(4\pi t/50), & t \geq 75, \end{cases} \tag{46}$$

The fault estimation results for rotor fault using the ATO are shown in Figs. 12 and 13. Figure 12 depicts the four estimation residuals for the corresponding rotors. As the sine wave offset fault signal is injected into F_2, it can be seen that only residual F_2 indicates a sine magnitude value close to 2000, which is the magnitude value of the fault signal, while the residuals F_1, F_3 and F_4 are all close to zero, which means that there is no fault in the three rotors. Accordingly, this result can be used to isolate the faulty rotor.

The comparison between fault estimation and the fault signal is shown in Fig. 13. It can be seen that the estimation has good convergence to the fault signal and

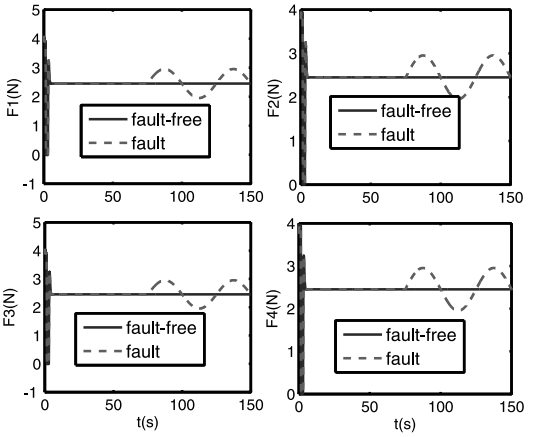

Fig. 11. Motor outputs in the case of a time-varying LOE fault $f_2 = 1/50$ Hz.

a relatively high accuracy for estimation. As it is not directly estimated and the estimate of the motor output F is derived from the estimation of the system input U, it has a small error for numerical calculations, but it is still suitable to provide useful information for AFTC.

Remark 2. The simulation results for fault scenarios 1 and 2 demonstrate the fault estimation results for different fault injection ways with different time-varying natures. Although the faults considered are additive, it is easy to transform them into multiplicative faults by changing the fault matrix F with reference to the matrix B in (10). Actually, the fault considered here is a kind of multiplicative fault with a 20% performance drop, but it is injected in the format of an additive fault. From both scenarios it can be seen that the improved ATO can estimate the fault offset parameters accurately, which could be used for AFTC of quadrotors.

5.1.3. Fault scenarios with disturbance and noise. In order to simulate the real-world scenario more closely and show the effectiveness of the proposed FE scheme affected by noise and disturbance, we simulate two fault scenarios with disturbance and noise. The sensor noise and actuator disturbance are individually injected to the quadrotor UAV model, together with the time-varying LOE fault $f_2 = 1/50$ Hz. The FE result subjected to the actuator disturbance is shown in Fig. 14. The actuator disturbance injected here is a band-limited white noise with power $P = 0.001$. From the FE result we can see that the FE can still track the real fault value under actuator disturbance. The FE result subjected to the sensor noise is shown in Fig. 15. The sensor noise is injected into the measurement of the quadrotor altitude. The noise injected here is also a band-limited white noise with power $P = 0.0001$. From the FE result we can see that the FE scheme can still track the real fault under sensor noise.

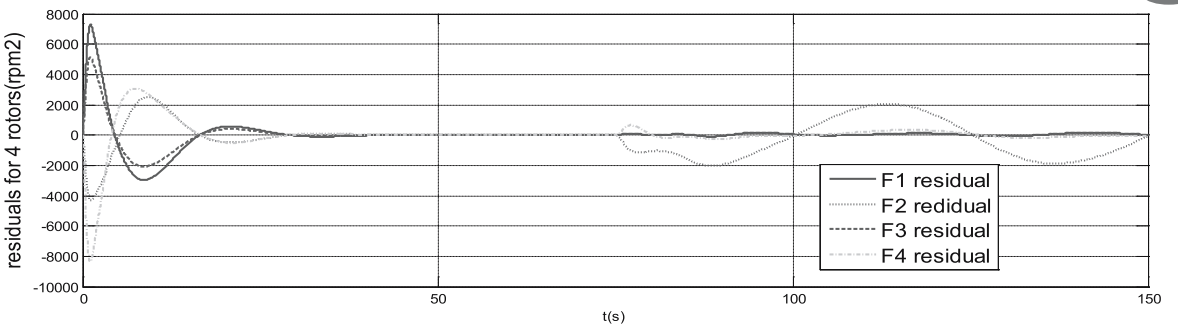

Fig. 12. FE residuals for four rotors.

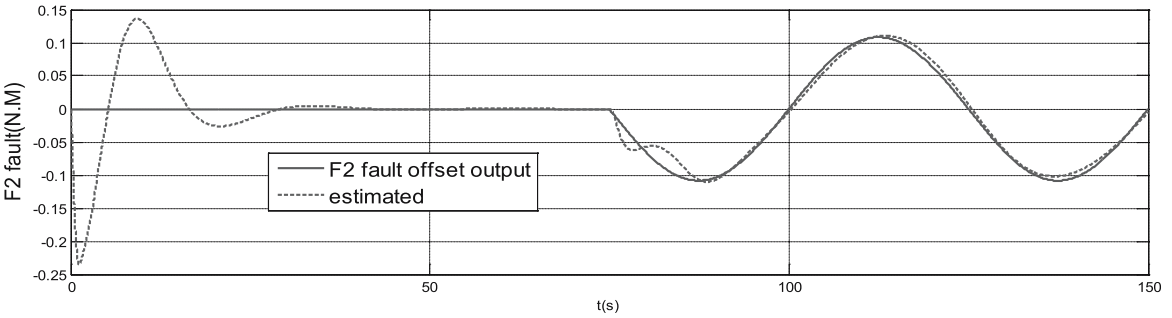

Fig. 13. Comparison between the fault estimate and the fault offset signal.

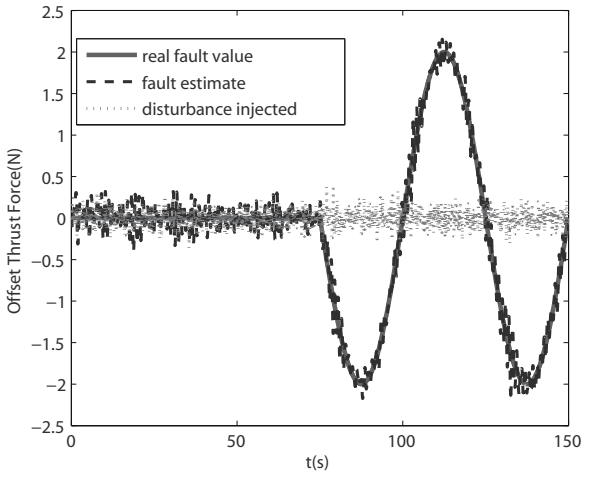

Fig. 14. Fault estimation subjected actuator disturbances.

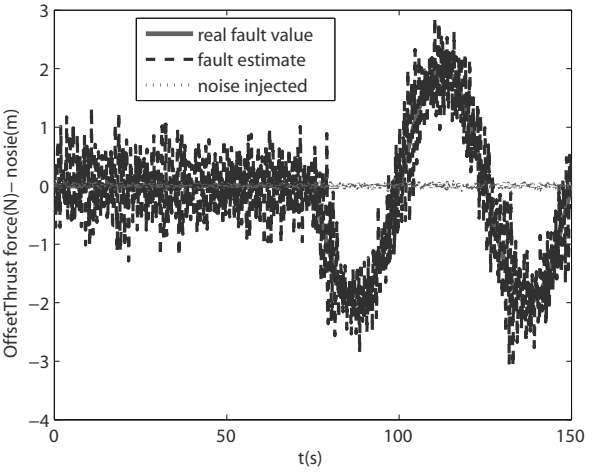

Fig. 15. Fault estimation subjected sensor noise.

Remark 3. Because of the observer's feedback effect, the FE scheme has some margin to tolerate the influence of noise and disturbance with low power. Where noise and disturbance with large power exist, some filter-based or disturbance-estimation based approaches are conventionally suggested for accommodation.

5.2. Systematic FTC simulation result. For the sake of generality, a rectangle trajectory (15 m $\times$ 15 m with a height of 10 m), as shown in Fig. 16, is designed to validate the FTC method. The flight simulation time is 300 seconds. The sine wave faults with different magnitudes are injected into U_1 for thrust force of the four rotors between 115 s and 185 s. Four levels of fault severity are considered for comparison. The first one corresponds to the fault-free case, the second one to a slight failure case with the fault between 150 s and 185 s, and the third one to a serious failure case with the fault

between 115 s and 128 s, while the last one to a fatal failure case with the fault between 130 s and 135 s.

Numerical simulations for different fault magnitudes with a limited number of discontinuous values were conducted. The fault tolerance capacity bounds for different FTC instances for U_1 fault are listed in Table 1.

The normal control result in the fault-free case is shown in Fig. 16. As can be seen, the normal PID controller allows the quadrotor to track the reference trajectory well.

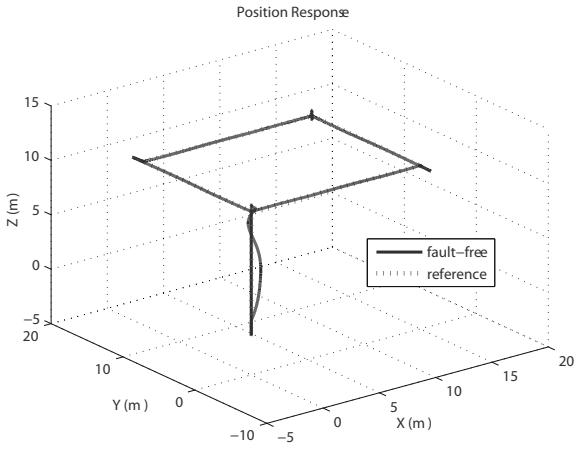

Fig. 16. Control trajectory in a fault-free case.

A comparison of control effects in the slight fault case is shown in Figs. 17 and 18. As can be seen from Fig. 17, all the control approaches can still track the trajectory well in the case of a slight fault, although it is subjected to the influence of the fault.

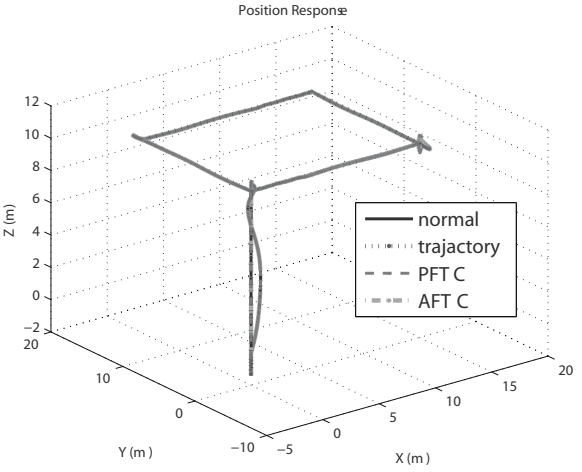

Fig. 17. Different FTC instances in a slight fault case.

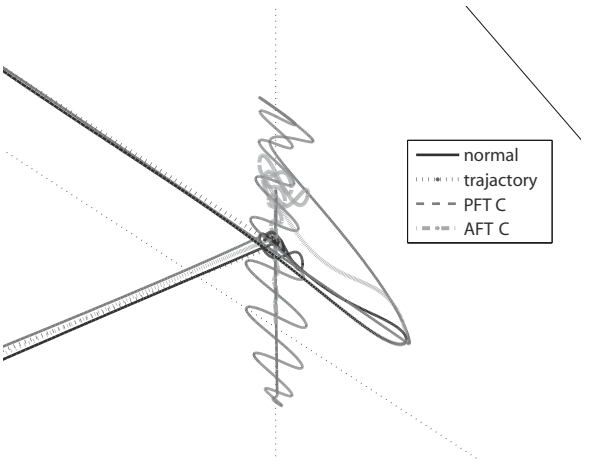

Fig. 18. Amplification of Fig. 17 during the fault period in a slight fault case.

As shown in Fig. 18, compared with the fault-free case, PFTC and AFTC in the slight failure case will lose some stability during the fault period, and AFTC is slightly better than PFTC, but it needs the information provided by the fault diagnosis. Accordingly, for the slight failure case, PFTC will be the optional control approach.

Control effects in the serious failure case without AFTC are shown in Fig. 19. As can be noticed, the quadrotor lost control in both the normal control and PFTC conditions.

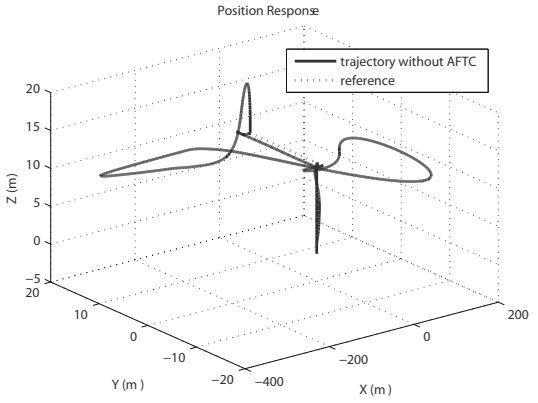

Fig. 19. Trajectory in a serious fault case without AFTC.

Control effects in the serious failure case with AFTC are shown in Fig. 20. As can be seen, AFTC can track the trajectory well in the serious failure case, and the fault can be compensated for, although there exists some disturbance. In consequence, this means AFTC works in the serous failure case and it is an optional control approach.

The fault parking result for the thrust fault can be seen in Fig. 21. The fault is detected at 130 s, and its value exceeds the tolerant bound 10 N of AFTC at about 132 s.

Table 1. Fault tolerant capacity bound for fault U_1.

Boundary	Normal controller	PFTC	AFTC	Fault parking
Upper bound	3	6	10	*
Lower bound	−3	−6	−10	*

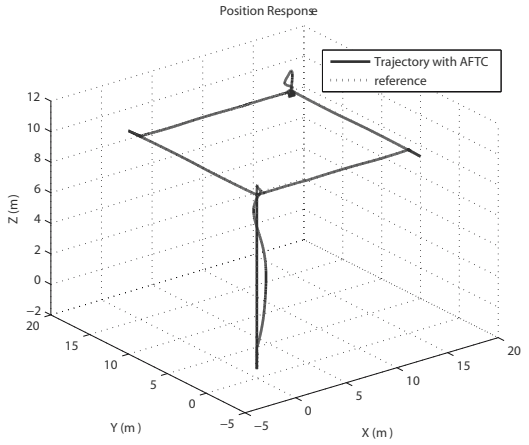

Fig. 20. Trajectory in a serious fault case with AFTC.

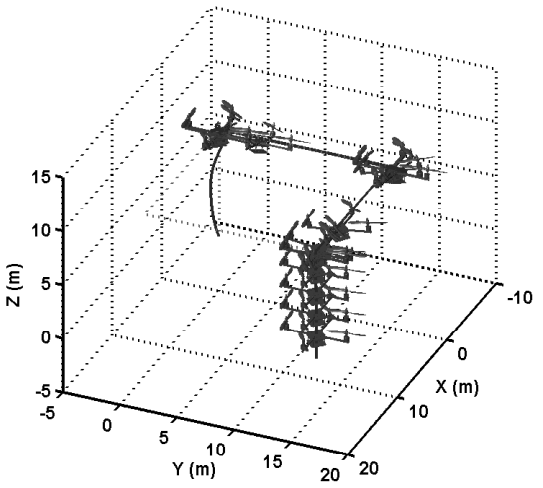

Fig. 21. Fault parking when AFTC lost control.

When the fault exceeds the AFTC bound, a freezing and hovering control strategy is adopted to stabilize the faulty quadrotor first. After the quadrotor becomes stable, a vertical land strategy is employed to landing the quadrotor under the control. Finally, a measure of powering off all the rotors is taken to avoid fatal crashes. the altitude status during fault parking can be seen in Fig. 22, while the effect on U_1 from fault injection and fault compensation can be seen in Figs. 23 and 24. Figure 22 depicts the fact the fact that the quadrotor enters into hovering mode at 132 s because the fault exceed the bound of 10 N, and then enter into landing mode at 137 s with the landing speed of 0.5 m/s. From the plots of landing velocity and angularity, we can see than it can land slowly with a specified velocity. Figures 23 and 24 show that fault compensation based on fault estimation can work before and after the fault exceeds the tolerant bound.

6. Conclusions

This paper proposed a systematic FTC strategy for the quadrotor based on the fault estimation result. In this scheme, the fault-tolerance capacities are innovatively defined, and then faults are classified into different levels based on the fault estimation result in order to choose the most suitable FTC control strategy to compensate for faults. The simulation result of the quadrotor flying in different fault cases demonstrates the performance and effectiveness of the proposed method. A further FTC control strategy for more complex faults is being developed. Future work will consider testing this method on a real flight in real time.

Acknowledgment

This work was supported by the UAE University under Grant 31N102.

References

Berbra, C., Lesecq, S. and Martinez, J. (2008). A multi-observer switching strategy for fault-tolerant control of a quadrotor helicopter, *16th Mediterranean Conference on Control and Automation, 2008, Ajaccio, France*, pp. 1094–1099.

Bouadi, H., Bouchoucha, M. and Tadjine, M. (2007). Sliding mode control based on backstepping approach for an UAV type-quadrotor, *International Journal of Mechanical, Aerospace, Industrial and Mechatronics Engineering* **1**(2): 22–27.

Boussaid, B., Aubrun, C., Abdelkrim, M.N. and Ben Gayed, M.K. (2011). Performance evaluation based fault tolerant control with actuator saturation avoidance, *International Journal of Applied Mathematics and Computer Science* **21**(3): 457–466, DOI: 10.2478/v10006-011-0034-x.

Chamseddine, A., Zhang, Y. and Rabbath, C.A. (2012). Trajectory planning and re-planning for fault tolerant formation flight control of quadrotor unmanned aerial vehicles, *American Control Conference (ACC), 2012, Montreal, QC, Canada*, pp. 3291–3296.

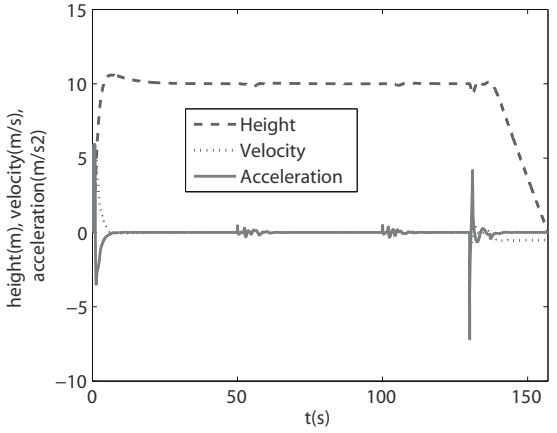

Fig. 22. Altitude status during fault parking.

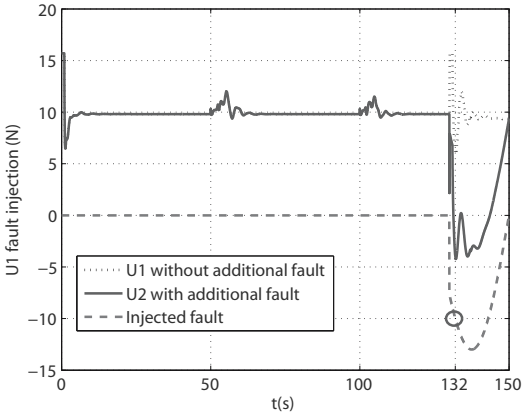

Fig. 23. Effect on U_1 from fault injection.

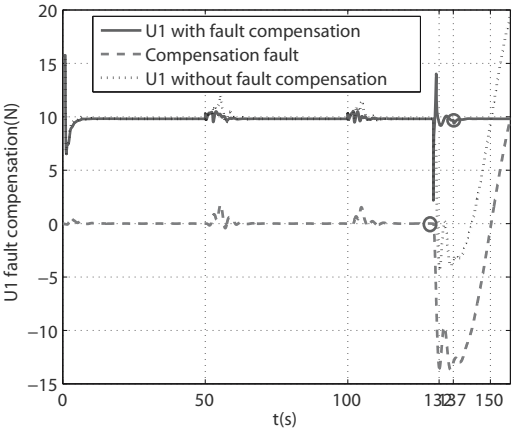

Fig. 24. Effect on U_1 from fault compensation.

Chen, J. and Patton, R.J. (1999). *Robust Model-based Fault Diagnosis for Dynamic Systems*, Kluwer, Boston, MA.

Du, M., Gandhi, R. and Mhaskar, P. (2011). An integrated fault detection and isolation and safe-parking framework for networked process systems, *Industrial & Engineering Chemistry Research* **50**(9): 5667–5679.

Du, M. and Mhaskar, P. (2011). A safe-parking and safe-switching framework for fault-tolerant control of switched nonlinear systems, *International Journal of Control* **84**(1): 9–23.

Edwards, C., Alwi, H. and Tan, C.P. (2012). Sliding mode methods for fault detection and fault tolerant control with application to aerospace systems, *International Journal of Applied Mathematics and Computer Science* **22**(1): 109–124, DOI: 10.2478/v10006-012-0008-7.

Fang, S. and Blanke, M. (2011). Fault monitoring and fault recovery control for position-moored vessels, *International Journal of Applied Mathematics and Computer Science* **21**(3): 467–478, DOI: 10.2478/v10006-011-0035-9.

Freddi, A., Longhi, S. and Monteriu, A. (2009). A model-based fault diagnosis system for a mini-quadrotor, *7th Workshop on Advanced Control and Diagnosis, Bari, Italy*, pp. 19–20.

Freddi, A., Longhi, S. and Monteriù, A. (2012). A diagnostic Thau observer for a class of unmanned vehicles, *Journal of Intelligent & Robotic Systems* **67**(1): 61–73.

Gandhi, R. and Mhaskar, P. (2008). Safe-parking of nonlinear process systems, *Computers & Chemical Engineering* **32**(9): 2113–2122.

Gandhi, R. and Mhaskar, P. (2009). A safe-parking framework for plant-wide fault-tolerant control, *Chemical Engineering Science* **64**(13): 3060–3071.

Izadi, H.A., Zhang, Y. and Gordon, B.W. (2011). Fault tolerant model predictive control of quad-rotor helicopters with actuator fault estimation, *World Congress, Milan, Italy*, Vol. 18, pp. 6343–6348.

Jiang, B. and Chowdhury, F.N. (2005). Fault estimation and accommodation for linear MIMO discrete-time systems, *IEEE Transactions on Control Systems Technology* **13**(3): 493–499.

Jiang, B., Staroswiecki, M. and Cocquempot, V. (2006). Fault accommodation for nonlinear dynamic systems, *IEEE Transactions on Automatic Control* **51**(9): 1578.

Jiang, B., Zhang, K. and Shi, P. (2011). Integrated fault estimation and accommodation design for discrete-time Takagi–Sugeno fuzzy systems with actuator faults, *IEEE Transactions on Fuzzy Systems* **19**(2): 291–304.

Khebbache, H., Sait, B. and Yacef, F. (2012). Robust stabilization of a quadrotor aerial vehicle in presence of sensor failures, *International Journal of Control Theory and Computer Modeling* **2**(2): 39–52.

Khelassi, A., Theilliol, D. and Weber, P. (2011). Reconfigurability analysis for reliable fault-tolerant control design, *International Journal of Applied Mathematics and Computer Science* **21**(3): 431–439, DOI: 10.2478/v10006-011-0032-z.

Li, T., Zhang, Y. and Gordon, B. (2011). Fault tolerant control applied to a quadrotor unmanned helicopter, *Proceedings of the 7th ASME/IEEE International Conference on*

Mechatronics & Embedded Systems & Applications, Washington, DC, USA, pp.1013–1022.

Mahmood, M., Gandhi, R. and Mhaskar, P. (2008). Safe-parking of nonlinear process systems: Handling uncertainty and unavailability of measurements, *Chemical Engineering Science* **63**(22): 5434–5446.

Meng, L., Jiang, B. and Xu, Y. (2009). Observer-based robust fault diagnosis for a class of uncertain nonlinear systems, *Chinese Control and Decision Conference, 2009, CCDC'09, Guilin, China*, pp. 885–889.

Montes de Oca, S., Puig, V., Witczak, M. and Dziekan, Ł. (2012). Fault-tolerant control strategy for actuator faults using LPV techniques: Application to a two degree of freedom helicopter, *International Journal of Applied Mathematics and Computer Science* **22**(1): 161–171, DOI: 10.2478/v10006-012-0012-y.

Pedro, J.O., Panday, A. and Dala, L. (2013). A nonlinear dynamic inversion-based neurocontroller for unmanned combat aerial vehicles during aerial refuelling, *International Journal of Applied Mathematics and Computer Science* **23**(1): 75–90, DOI: 10.2478/amcs-2013-0007.

Ranjbaran, M. and Khorasani, K. (2010). Fault recovery of an under-actuated quadrotor aerial vehicle, *49th IEEE Conference on Decision and Control (CDC), 2010, Atlanta, GA, USA*, pp. 4385–4392.

Sadeghzadeh, I., Mehta, A., Zhang, Y. and Rabbath, C.-A. (2011). Fault-tolerant trajectory tracking control of a quadrotor helicopter using gain-scheduled PID and model reference adaptive control, *Annual Conference of the Prognostics and Health Management Society, Montreal, Canada,* Vol. 2, pp. 1–10.

Sharifi, F., Mirzaei, M., Gordon, B. W. and Zhang, Y. (2010). Fault tolerant control of a quadrotor UAV using sliding mode control, *Conference on Control and Fault-Tolerant Systems (SysTol), 2010, Nice, France*, pp. 239–244.

Theilliol, D., Join, C. and Zhang, Y. (2008). Actuator fault tolerant control design based on a reconfigurable reference input, *International Journal of Applied Mathematics and Computer Science* **18**(4): 553–560, DOI: 10.2478/v10006-008-0048-1.

Yang, H., Jiang, B., Cocquempot, V. and Lu, L. (2012). Supervisory fault tolerant control with integrated fault detection and isolation: A switched system approach, *International Journal of Applied Mathematics and Computer Science* **22**(1): 87–97, DOI: 10.2478/v10006-012-0006-9.

Zhang, K., Jiang, B. and Shi, P. (2007). Adaptive observer-based fault diagnosis with application to satellite attitude control systems, *Second International Conference on Innovative Computing, Information and Control, 2007, Kumamoto, Japan*, pp. 508–508.

Zhang, Y. and Chamseddine, A. (2012). Fault tolerant flight control techniques with application to a quadrotor UAV testbed, *in* T. Lombaerts (Ed.), *Automatic Flight Control Systems—Latest Developments*, InTech, Rijeka, pp. 119–150.

Zhang, Y. and Jiang, J. (2003). Bibliographical review on reconfigurable fault-tolerant control systems, *Proceedings of the 5th IFAC Symposium on Fault Detection, Supervision and Safety for Technical Processes 2003, Washington, DC, USA*, pp. 265–276.

Zhang, Y. and Jiang, J. (2008). Bibliographical review on reconfigurable fault-tolerant control systems, *Annual Reviews in Control* **32**(2): 229–252.

Zhaohui, C. and Noura, H. (2013a). An adaptive Thau observer for estimating the time-varying LOE fault of quadrotor actuators, *Conference on Control and Fault-Tolerant Systems (SysTol), 2013, Nice, France*, pp. 468–473.

Zhaohui, C. and Noura, H. (2013b). A composite fault tolerant control based on fault estimation for quadrotor UAVs, *Conference on Industrial Electronics and Applications (ICIEA), 2013 8th, Melbourne, Australia*, pp. 236–241.

Zhaohui, C., Noura, H., Susilo, T.B. and Al Younes, Y. (2013a). Engineering implementation on fault diagnosis for quadrotors based on nonlinear observer, *25th Chinese Control and Decision Conference (CCDC), 2013, Guiyang, China*, pp. 2971–2975.

Zhaohui, C., Noura, H., Susilo, T.B. and Al Younes, Y. (2013b). Robust fault diagnosis for quadrotor UAVs using adaptive Thau observer, *Journal of Intelligent & Robotic Systems* **73**(1–4): 1–16.

Zhaohui, C., Noura, H. and Younes, Y.A. (2013c). Robust fault estimation on a real quadrotor UAV using optimized adaptive Thau observer, *2013 International Conference on Unmanned Aircraft Systems (ICUAS), Atlanta, GA, USA*, pp. 550–556.

Zhaohui Cen received his B.Sc. (in telecommunication engineering), M.Sc. (in information and telecommunication systems) and Ph.D. (in information and telecommunication systems) degrees from the Department of Electronics and Information Engineering, Huazhong University of Science and Technology, China, in 2005, 2007, 2011, respectively. From 2012 to 2013, he worked as a research associate at United Arab Emirates University, the University of Sheffield (UK), and the University of Lincoln. Currently, he is a research engineer of electronics at the Qatar Environment and Energy Research Institute (QEERI), a member of the Qatar Foundation, Qatar. His research interests are in the field of measurement and control, especially condition monitoring and control for aircraft and power systems. His current research at the QEERI focuses on smart micro-grids for renewable energy integration based on power electronics and embedded system technologies.

Hassan Noura received his Master's and Ph.D. degrees in automatic control from University Henri Poincaré, Nancy 1, France, in 1990 and 1993. He obtained his habilitation to supervise research in automatic control at University Henri Poincaré, Nancy 1, in 2002. He was an associate professor in this university from 1994 to 2003. In 2003, he joined Paul Cézanne University, Aix-Marseille III, France, as a professor of control systems. Currently, he is a professor at United

Arab Emirates University, Department of Electrical Engineering (since 2007). His research fields of interest are mainly control systems, fault diagnosis and fault tolerant control.

Younes Al Younes received his M.Sc. degree from the Department of Mechanical Engineering, American University of Sharjah, UAE, in 2007. Currently, he is at the Mechanical Engineering Faculty at the Higher Colleges of Technology, Al Ain, UAE, and a Ph.D. student at the University of Picardie Jules Verne, Amiens, France. His research fields of interest are mainly control and fault diagnosis for quadrotors.

Received: 13 February 2014
Revised: 1 July 2014